IOPscience iopscience.iop.org

Home Search Collections Journals About Contact us My IOPscience

Thermodynamic stability and electronic structure of small carbon nitride nanotubes

This article has been downloaded from IOPscience. Please scroll down to see the full text article.

2009 J. Phys.: Condens. Matter 21 144203

(http://iopscience.iop.org/0953-8984/21/14/144203)

View the table of contents for this issue, or go to the journal homepage for more

Download details:
IP Address: 129.252.86.83
The article was downloaded on 29/05/2010 at 18:55

Please note that terms and conditions apply.

IOP Publishing Journal of Physics: Condensed Matter

J. Phys.: Condens. Matter **21** (2009) 144203 (7pp) doi:10.1088/0953-8984/21/14/144203

Thermodynamic stability and electronic structure of small carbon nitride nanotubes

John Hales[1] **and Amanda S Barnard**[2]

[1] Division of Biosciences, University College London, Gower Street, London, WC1E 6BT, UK
[2] School of Chemistry, University of Melbourne, Parkville, Victoria, Australia

E-mail: john.hales@ucl.ac.uk and amanda.barnard@unimelb.edu.au

Received 5 June 2008
Published 18 March 2009
Online at stacks.iop.org/JPhysCM/21/144203

Abstract

In order to tune the electronic properties of carbon-based nanotubes, attention is now turning to new avenues based on chemical manipulation. The introduction of nitrogen at either doping or alloying concentrations has been shown to give rise to new tubular structures and desirable electronic properties, but a detailed understanding of the strain and thermodynamic properties is still lacking. In this paper a systematic computational study of the structure and thermodynamics of small C_xN nanotubes is presented ($x = 1$, 2, 3, 5, and 7). The aim of this work is to investigate which stoichiometries and atomic distributions are likely to be stable under ambient and operating conditions, thereby offering viable candidates for future synthesis efforts. In addition to this, the electronic properties of stable structures are briefly examined, to establish whether small carbon nitride nanotubes may be tailored for emerging technological applications.

(Some figures in this article are in colour only in the electronic version)

1. Introduction

From the early 1990s carbon nanotubes (CNTs) have stimulated considerable interest worldwide, and have shown great potential for a variety of technological applications [1–3]. Due to their superior electronic and mechanical properties, carbon nanotubes have been seen as the optimal choice of one-dimensional structures for the next generation of electronic devices at the nanoscale [4]. The linear dimensionality of CNTs may also give rise to other useful phenomena, and specific CNTs exhibit exotic Luttinger-liquid behaviour rather than the usual Fermi-liquid behaviour, making them 'quantum wires' [5]. Not surprisingly, much attention has been focused on developing CNT-based nanoscale components [3]. However, a major obstacle that hinders actualization of CNT-based nanodevices is that as-grown carbon nanotubes exhibit a range of different chiralities [6]. At this stage, there is no reliable and *commercially viable* method of separating CNTs according to their electronic properties. Therefore, if nanotube-based nanotechnology is to continue to progress, it is necessary to consider alternative methods of tailoring the electronic properties.

An alternative route to the production of nanotubes with tailor-made electronic properties, based on chemical manipulation, is to inject charges into the system artificially [7–9]. Like conventional semiconductors, the electronic properties of CNTs may be modified by introducing a small concentration of impurities, such as substitutional nitrogen [10]. However, while studying $C_{13}N_x$ and $C_{49}N_x$ ($x \leqslant 1$) nanofibres, Terrones *et al* [11, 12] concluded that it was difficult to create highly ordered carbon networks with large quantities of nitrogen, and that the nitrogen incorporation was responsible for the high degree of tubular imperfection that was observed. More recently, Li *et al* [13] have synthesized C_3N_4 nanobelts and nanotubes using a solvothermal method, but concluded that the electronic and other properties of these nanotubes required further investigation. Previously reported quantum chemical studies indicate that CN nanotubes are metallic, but that the precise nature of the optoelectronic properties depends on the atomic structure and specifically on the type of nitrogen incorporation. Collectively these studies point to the possibility of tuning the electronic and chemical properties via changes in the stoichiometry of the C_xN_y composition and the type of C–N distributions in the nanotubes [14].

 © 2009 IOP Publishing Ltd Printed in the UK

This avenue of research has already shown some promise, but clearly if some of the potentially exciting properties of C_xN_y nanotubes are to be exploited, a detailed knowledge of the structural stability and electronic properties of these materials is imperative. To date, no systematic study has been undertaken examining all important properties that definitely identifies which properties are realistically controllable and which are not. For example, although there is reliable evidence that carbon nitride nanotubes (with closer to equivalent amounts of C and N) may be an ideal alternative to CNTs, no calculations of the strain energy or thermodynamic properties have been reported. This is an ideal problem for theoretical and computational methods, and motivates the present study that focuses on C_xN nanotubes with $x = 1$, 2, 3, 5, and 7.

In this paper density functional tight-binding calculations are used to model the structure and thermodynamic properties of these C_xN nanotubes to determine which stoichiometries and which atomic distributions are stable, and therefore viable candidates for future synthesis efforts. In the proceeding sections each of these structural aspects is discussed separately. In general, the results predict that the stability of C_xN nanotubes is highly dependent on the stoichiometry and the nitrogen partial pressure (during synthesis), but is almost independent of chiral structure. In addition to this, we show that there is a relatively constant blue-shift in the Fermi energy when $2 < x$.

2. Methodology

The density functional based tight-binding method with self-consistent charges (SCC-DFTB) [15, 16] is a two-centre approach to density functional theory (DFT), where the Kohn–Sham density functional is expanded to second order around a reference electron density. The reference density is obtained from self-consistent density functional calculations of weakly confined neutral atoms, and the confinement potential is optimized to anticipate the charge density and effective potential in molecules and solids. A minimal valence basis is established and one- and two-centre tight-binding matrix elements are explicitly calculated within DFT. A universal short-range repulsive potential accounts for double counting terms in the Coulomb and exchange–correlation contributions, as well as the internuclear repulsion, and self-consistency is included at the level of Mulliken charges, as described in [16]. This method has been selected for use here as it has previously been shown to provide good agreement with higher level quantum chemical methods and density functional theory for carbon–nitrogen systems [17–19] to an excellent energy resolution. In the present study, all test structures were fully relaxed using the conjugate gradient scheme to minimize the total energy with the convergence criterion for a stationary point at 10^{-4} au $\approx$ 5 meV Å^{-1} for forces. Preliminary tests of k-point density we undertaken, and it was determined the 12 k-points along the periodic principle axis of the simulation segment were sufficient to achieve energetic convergence with this stationary point.

3. Discussion of results

3.1. Structural stability

In general, the C_xN nanotube structures examined here may be described in terms of their chirality (n, m) and stoichiometry x. During our study we have used a structure set with $n = 4$, 5, 6, 7, 8, 9, $m = 0$ (zig-zag) and $m = n$ (armchair), and with stoichiometry $x = 1$, 2, 3, 5 and 7. Although the structures produced with these geometries should provide the full range of possible properties, in addition to this, we have also sampled a number of different atomic configurations, or 'substitution patterns' for N atoms in a C nanotube. Since there is no experimental evidence as to the spatial distribution of N in N-doped CNTs or C_xN nanotubes, we have sampled a number of different patterns and attempted to ascertain if particular configurations are more stable. Based on previous studies of boron nitride nanotubes [20] we expect that N–N bonds will be unstable, and have therefore categorized the substitution patterns according to the proximity of N atoms to other N atoms in the lattice.

The nomenclature used to identify the four main substitution patterns are s, h, n and c, which refer to N atoms that are distributed in 'spaced', 'helical', 'neighbouring' and 'chain' configurations (relative to each other), respectively. In a 'spaced' pattern, the nitrogen atoms do not neighbour one another (there are no N–N bonds) and there is a homogeneous distribution of N atoms around the nanotube that does not reflect the underlying chiral structure. In a 'helical' pattern the nitrogen atoms do not neighbour one another (there are no N–N bonds) but the distribution of N atoms around the nanotube does reflect the chiral structure, and is clearly evident as a helix pattern wrapping about the nanotube. In a 'neighbouring' pattern, there is a homogeneous distribution of N atoms about the nanotube (that does not reflect chiral structure), but each N atom is first nearest neighbours with at least one other N atom (there are N–N bonds). And finally, in a 'chain' pattern the nitrogen atoms neighbour one another, and the distribution of N atoms around the nanotube reflects chiral structure, like an infinite –N–N–N– chain around the nanotube. The B_2N and BN_2 nanotubes in [20] are examples of chain patterns. It is important to point out that these categories may not be sufficient to describe the full range of substitution patterns that may be observed experimentally. Therefore, in a small number of cases, we have also included some more random configurations that fall between (or in) two categories, such as s, n and h, n. In the case of an s, n pattern, pairs of N atoms are spaced around the nanotube, and in h, n a helical pattern that includes some pairs of N atoms is sampled.

Examples showing how these substitution patterns may relate to the of the stoichiometry are given in figure 1 for the subset of (6, 0) nanotubes used in this study. To the left is a pure C nanotube (for comparison) and then the remaining C_xN nanotubes with increasing N content ($x = 7$, 5, 3, 2, 1 from left to right). In these cases the C_7N and CN nanotubes have spaced s patterns, and the C_5N, C_3N and C_2N nanotubes have helical h patterns[3]. The inclusion of this range

[3] Alternative patterns are illustrated in figure 2.

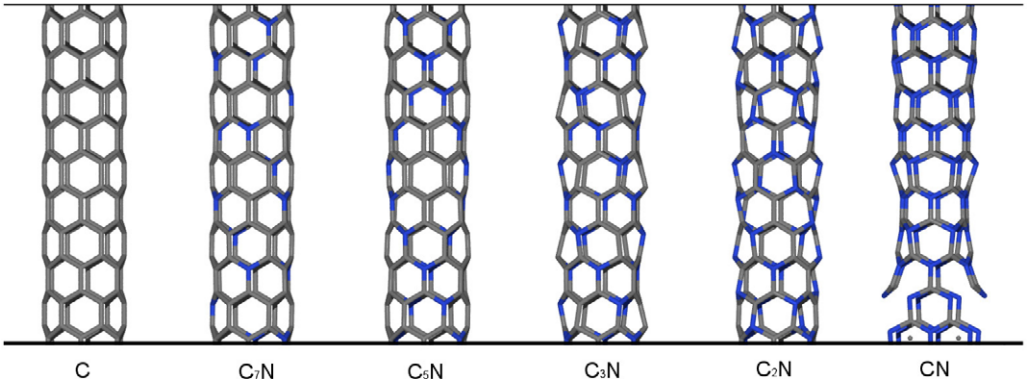

Figure 1. The relaxed structures of the (6, 0) nanotubes, with increasing N content (left to right). The substitution patterns for the N atoms are *s*, *h*, *h*, *h* and *s* for the C_7N, C_5N, C_3N, C_2N and CN nanotubes, respectively. The relaxed structures categorized as *cylindrical*, *cylindrical*, *distorted*, *distorted*, and *winged*, respectively.

Table 1. The substitution pattern of nitrogen in C_xN nanotubes, and the categorization of structural stability for the final, relaxed structures (*pattern* | *relaxed structure category*). The substitution patterns *s*, *h*, *n* and *c* refer to N atoms that are distributed in 'spaced', 'helical', 'neighbouring' and 'chain' configurations (relative to each other), respectively.

n	*m*	C_7N	C_5N	C_3N	C_2N	CN
4	0	*h* | *cylindrical*	*h* | *cylindrical*	*h* | *cylindrical*	*n* | *winged*	*s* | *cylindrical*
5	0	*h* | *cylindrical*	*s* | *cylindrical*	*h* | *winged*	*n* | *broken*	*s* | *winged*
6	0	*s* | *cylindrical*	*h* | *cylindrical*	*h* | *distorted*	*h* | *distorted*	*s* | *winged*
7	0	*h* | *cylindrical*	*s* | *cylindrical*	*h* | *distorted*	*n* | *broken*	*h* | *winged*
8	0	*h* | *cylindrical*	*s* | *cylindrical*	*h* | *distorted*	*n* | *distorted*	*s* | *distorted*
9	0	*h* | *cylindrical*	*h* | *cylindrical*	*h* | *distorted*	*h* | *broken*	*s* | *distorted*
4	4	*h* | *distorted*	*s* | *broken*	*h* | *distorted*	*n* | *distorted*	*s* | *broken*
5	5	*s* | *distorted*	*h* | *broken*	*h* | *distorted*	*h*, *n* | *distorted*	*s* | *broken*
6	6	*s* | *cylindrical*	*h* | *cylindrical*	*h* | *distorted*	*c* | *broken*	*s* | *broken*
7	7	*h* | *distorted*	*s* | *distorted*	*h* | *distorted*	*s*, *n* | *distorted*	*s* | *broken*
8	8	*h* | *cylindrical*	*h* | *cylindrical*	*h* | *distorted*	*h*, *n* | *distorted*	*s* | *distorted*
9	9	*s* | *cylindrical*	*h* | *cylindrical*	*h* | *distorted*	*c* | *broken*	*s* | *distorted*

of atomic configurations is important to effectively sample morphology space, and provide results that will be comparable with the morphological ensemble of configurations that may be produced experimentally.

In addition to the different substitution patterns shown in figure 1, we can also see that the overall structure of the C_xN nanotubes changes (compared to the C nanotube) as the stoichiometry is varied. Structural changes such as these have also been categorized, in terms of these severity of the imperfection, in order to identify trends in the structural stability of the C_xN nanotubes. The nomenclature used to categorize the four main relaxed structure types are *cylindrical*, *distorted*, *broken* and *winged*, respectively. The *cylindrical* structures are those which have a structure similar to a pure C nanotube of the same chirality. In a *distorted* structure all of the interatomic bonds remain intact, but there are out-of-plane distortions resulting from changes in the torsional angles (as per the C_3N, C_2N (6, 0) nanotubes in figure 1). In a *broken* nanotube, either N–N or C–N bonds have broken following the structural relaxation, and there are changes in the bond lengths and bond angles surrounding the resultant defect. And finally, in a *winged* nanotube either N–N or C–N bonds are broken, and there are changes in the bond lengths, bond angles and torsional angles surrounding the defect, resulting in non-tubular protrusions. These protrusions similar to those observed in the carbon nanotubes with

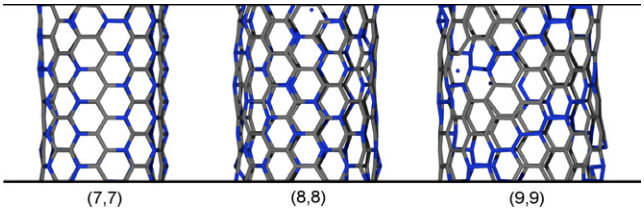

Figure 2. The relaxed structures of the C_2N (7, 7), (8, 8) and (9, 9) nanotubes. The substitution patterns are *s*, *n*, *h*, *n* and *c*, and the corresponding dominant (relaxed) structural categories are *distorted*, *distorted*, and *broken*, respectively. The single dots are free N atoms that have broken all bonds with neighbouring C and N atoms in the nanotube.

graphitic wings observed by Trasobares *et al* [21], and may contribute to the formation of bamboo structures observed experimentally [8, 22–25]. Further examples of some of the relaxed C_xN nanotubes are shown in figure 2.

Based on these categories for the substitution pattern and relaxed structure, table 1 lists all of the results for each combination of (n, m) and C_xN. We can see from this table that the structures deteriorate with decreasing x (or increasing N content) as suggested by Terrones *et al* [11, 12]. In addition to this, we find that at low N concentrations $(n, 0)$ nanotubes are more likely to have fewer defects than (n, n) nanotubes. In general the relaxed C_3N nanotube exhibit the most consistent

Table 2. The fraction of relaxed C_xN nanotubes exhibiting *cylindrical*, *distorted*, *broken* and *winged* structures, depending upon the *s*, *h*, *n* or *c* nitrogen substitution pattern. The total fraction (irrespective of N substitution pattern) is given in the right column.

	s	*h*	*n*	*c*	Total
Cylindrical	31.8%	44.8%	0.0%	0.0%	19.2%
Distorted	31.8%	48.3%	57.1%	0.0%	34.3%
Broken	22.7%	3.4%	28.6%	100.0%	38.7%
Winged	13.6%	3.4%	14.3%	0.0%	7.8%

results, showing a similar *distorted* structure that is largely independent of the chiral index.

As a final comparison of the relationship between the patterning and structural deformities, table 2 presents the statistical results for all structures, irrespective of the (n, m) or x. We can see here that the helical distribution (and to a lesser extent, the *spaced* distribution) is most likely to result in *cylindrical* or *distorted* structures. Neighbouring N atoms will either result in *distorted* structures or broken N–N bonds, and the *chain* structure is highly unstable. Although table 2 indicates that protrusions characteristic of the *winged* structures are likely to be associated with neighbouring N atoms, we can see from table 1 that this type of defect is more likely due to the combination of small diameters and high N concentration than to any particular substitution pattern.

3.2. Thermodynamic stability

To determine whether or not the C_xN nanostructures described above are likely to form experimentally, and be stable under ambient conditions, the thermodynamic stability was assessed by considering the average binding energies of each structure. As outlined in [26], the average binding energy for sets of (n, m) nanotubes may be used to extract components associated with the strain (E_s) and cohesive (E_c) elements, due to the curvature induced bond bending and bond stretching, respectively. This may be achieved for each stoichiometry using the results in figure 3(a) and the simple expression:

$$\frac{E_{CN}(n,m)}{N} = E_s\frac{1}{R^2} + \frac{E_c}{N} \tag{1}$$

where N is the total number of atoms, R is the mean radius of curvature, and $E_{CN}(n, m)$ is the total energy of the C_xN nanotube with chirality (n, m), which we have calculated explicitly using SCC-DFTB. This gives us the values of the E_s (from the coefficient) and the E_c in the limit as the tube diameter $R \to \infty$. We can see in figure 3(b) how these values change with the fraction of N in the nanotubes, but more importantly we can use these values of E_c to estimate a chemical potential of an infinite (planar) sheet and hence the formation energy for each stoichiometric combination.

To be of use in experimental situations, an unambiguous definition of the formation energetics must be expressed in terms of the chemical potential or partial pressure of nitrogen (P_N). A simple definition of the nonstoichiometric formation energy of a two-component nanotube may be defined as

$$E_F(n,m) = E_{CN}(n,m) - N_C\mu_{C,tube} - N_N\mu_{N,gas}, \tag{2}$$

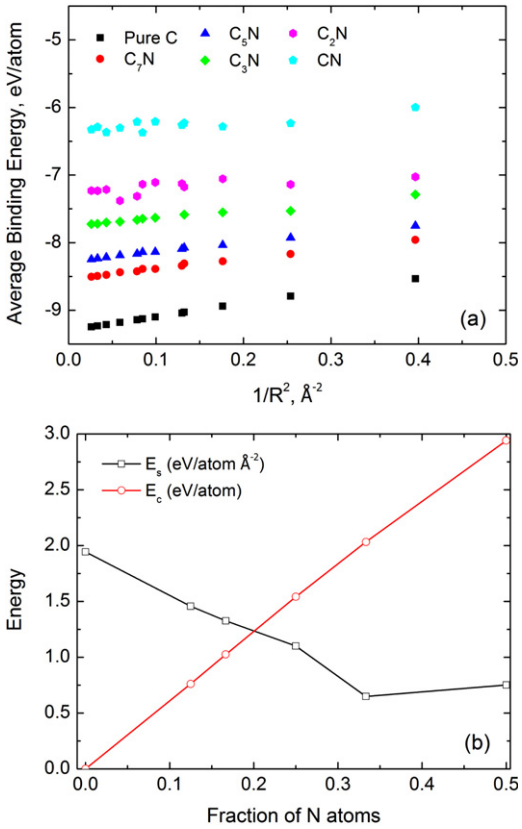

Figure 3. (a) The calculated average binding energy for all (n, m) nanotubes for each C_xN stoichiometry. (b) The strain energy E_s from the coefficient of the linear fits to (a), and the cohesive energy E_c from the intercepts of (a) as a function of the fraction of N atoms in the nanotubes.

where $E_{CN}(n, m)$ is the total energy of a fully relaxed nanotube with chiral index (n, m), $\mu_{C,tube}$ is the elemental chemical potential of C in a pure carbon nanotube, $\mu_{N,gas}$ is the elemental chemical potential of N in a gaseous N_2 molecule (also calculated using SCC-DFTB), and N_C and N_N are the number of carbon and nitrogen atoms in the system, respectively. For a C_xN nanotube to form, the structure must be in thermodynamic equilibrium with the individual components and comparable planar (sheet) structures, such as graphene (i.e., in the limit when $R \to \infty$). Therefore, at equilibrium the sum of the elemental chemical potentials will be equal to the chemical potential of an ideal C_xN sheet,

$$\mu_{C,tube} + \mu_{N,gas} = \mu_{CN,tube} = \mu_{CN,sheet} \tag{3}$$

and the formation energy will be

$$E_F(n,m) = E_{CN}(n,m) - N_C\mu_{CN,sheet} - (N_C - N_N)\mu_{N,gas}. \tag{4}$$

This may be expressed in terms of P_N by relating $\mu_{N,gas}$ to the chemical potentials of C and C_xN sheets, and introducing a free energy of formation ΔH_f, so that

$$\mu_{CN,sheet} = \mu_{C,sheet} + \mu_{N,gas} + \Delta H_f. \tag{5}$$

The free energy of formation is defined (in the limit) as above, or at equilibrium (from equation (3)) as $\Delta H_f = \mu_{CN,tube} -$

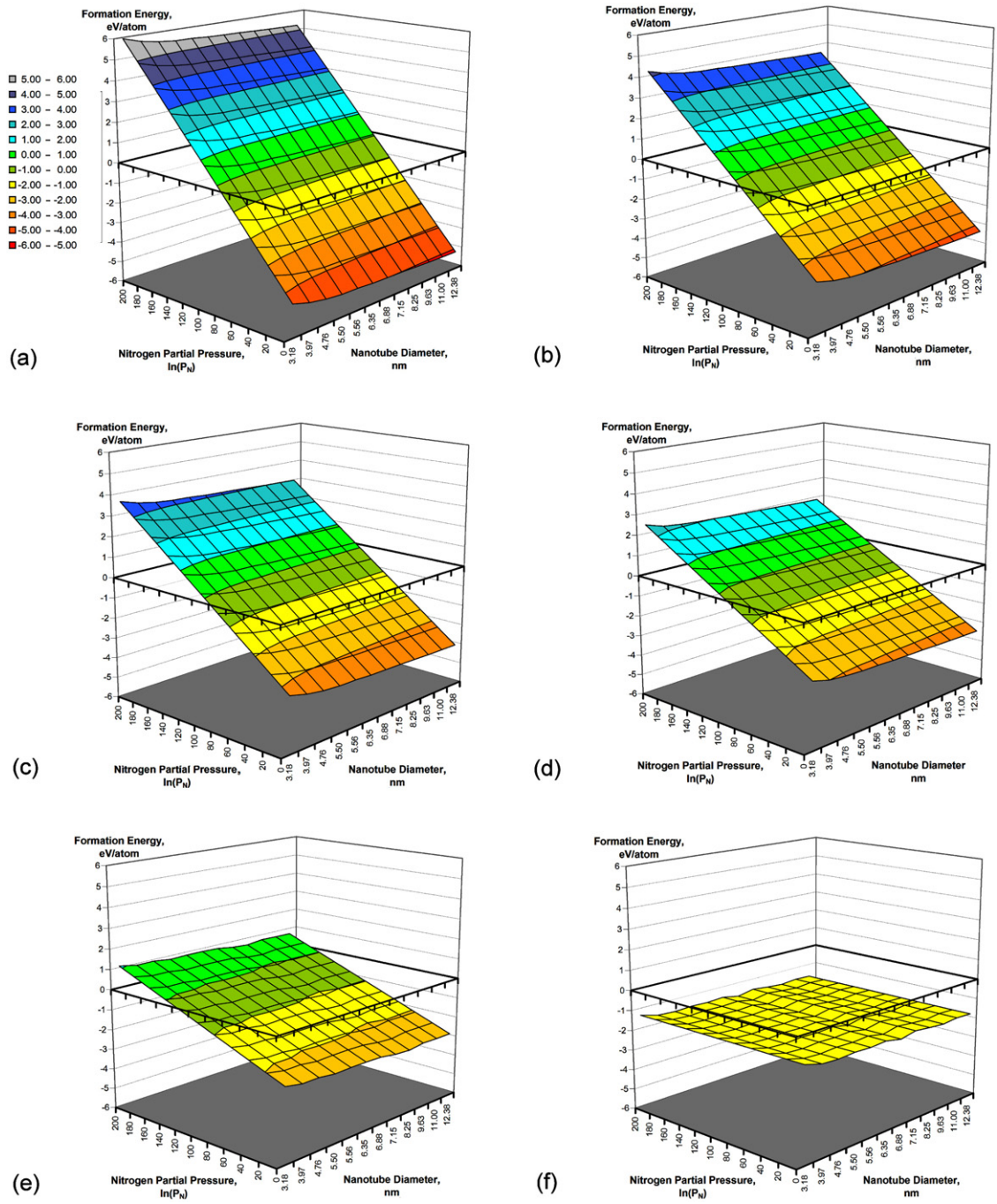

Figure 4. The calculated formation energies $E_F(T, n, m)$ at $T = 600$ K as a function of $D(n, m)$ and $\ln(P_N)$, for the (a) pure C, (b) C_7N, (c) C_5N, (d) C_3N, (e) C_2N, and (f) CN nanotubes.

$\mu_{C,tube} + \mu_{N,gas}$. This leaves the $\mu_{N,gas}$, which may be defined in terms of the standard state chemical potential:

$$\mu_{N,gas} = \mu^{\circ}_{N,gas} + kT\ln\left(\frac{P_N}{P^{\circ}_N}\right) = \mu^{\circ}_{CN,sheet} - \mu^{\circ}_{C,sheet} - \Delta H^{\circ}_f + kT\ln(P_N). \quad (6)$$

Using these definitions, we may define a formation energy for C_xN nanotubes of any chiral index:,

$$E_F(T, n, m) = E_{CN}(n, m) - N_C\mu_{CN,sheet} - (N_C - N_N) \times \left[\mu^{\circ}_{CN,sheet} - \mu^{\circ}_{C,sheet} - \Delta H^{\circ}_f\right] + (N_C - N_N)kT\ln(P_N). \quad (7)$$

We may also define the range of P_N, by prescribing that all N will be incorporated in to the tubes ($\mu_{N,gas} < \mu^{\circ}_{N,gas}$), that no graphene sheets will be formed ($\mu_{C,tube} < \mu_{C,sheet}$) and that in the limit $\Delta H^{\circ}_f = \mu_{CN,sheet} - \mu_{C,sheet} + \mu_{N,gas}$ (when $R \to \infty$). Hence, $0 < \ln(P_N) < \Delta H^{\circ}_f/kT$.

Naturally this expression and limiting criteria is entirely general, and would be equally applicable to C_xB_y nanotubes, B_xN_y nanotubes, or indeed any two-component nanotube system. In the present study we have used the coefficients from equation (1) shown in figure 3(b) as $\mu^{\circ}_{C,sheet}$ and $\mu^{\circ}_{CN,sheet}$ (our limiting cases) and the explicit data points in figure 3(a)

provide us with the values for $E_{CN}(n, m)$. The value for $\mu^{\circ}_{N,gas}$ required for the definition of ΔH°_{f} was taken from the energy per N atom in an N_2 dimer.

Using these values in combination with equation (7), we have plotted $E_F(T, n, m)$ for each stoichiometry at $T = 600$ K. For consistency, these results are shown over the range $200 > \ln(P_N) > 0$ in figures 4(a)–(f), for the pure C nanotubes ($x = \infty$), $x = 7, 5, 3, 2$ and 1, respectively. In these plots the results for $(n, 0)$ and (n, n) have been combined and the results plotted as a function of the nanotube diameter D, since $D(n, m)$. Beginning with figure 4(a), we can see that $E_F(600, n, m)$ is a minimum when $\ln(P_N) = 0$, irrespective of D. As we change the stoichiometry (figures 4(b)–(e)) the results remain largely independent of D, and the dependence on $\ln(P_N)$ is clearly evident. Finally, we can see in figure 4(f) that $E_F(600, n, m)$ is independent of $\ln(P_N)$, as we expect for the stoichiometric case, and the only variations in $E_F(600, n, m)$ are due to the structural changes described in section 3.1. These results indicate that the nitrogen partial pressure will be the critical factor in determining the stoichiometry of small carbon nitride nanotubes during growth, and little or no stoichiometric variations would be expected among nanotubes of different chiral structures. Unfortunately, no systematic experimental study of this type could be found for comparison.

3.3. Electronic properties

Once the structural and thermodynamic stability of possible C_xN nanotube has been addressed, an investigation of the electronic properties is necessary to determine if these nanostructures are likely to be useful in future applications, and therefore represent attractive candidates for future synthesis. The next generation of nanotube-based devices will require more than simply tunable electronic properties, it will also require reliable integration of singular components and the formation of reproducible superstructures. It has been shown by Peng *et al* [27] that it is possible to create compound nanotube systems in which 'T' junctions are formed as a results of narrow diameter nanotube growing at a defect site of a larger nanotube. However, if such junctions are to be useful electronically, it is desirable to know the Fermi energies of narrow nanotubes, so as to facilitate the design junctions with specific electronic properties.

Therefore, in response to the work by Peng *et al* [27], we have briefly examined the relationship between the C_xN stoichiometry and the Fermi energy for our (relaxed) small diameter nanotubes, over a range of $D(n, m)$. These results are presented in figure 5 where we can see that there is a relatively constant blue-shift of ∼1.5 eV in the Fermi energy when $2 < x$. The origin of this blue-shift is currently unknown, and is still under investigation. There are more unpredictable changes in the Fermi energy when $x \leqslant 2$, due to the various structural instabilities described in section 3.1. In general, the size dependence in the Fermi energy of the C_xN nanotubes (when $2 < x$) is consistent with that observed for all C nanotubes.

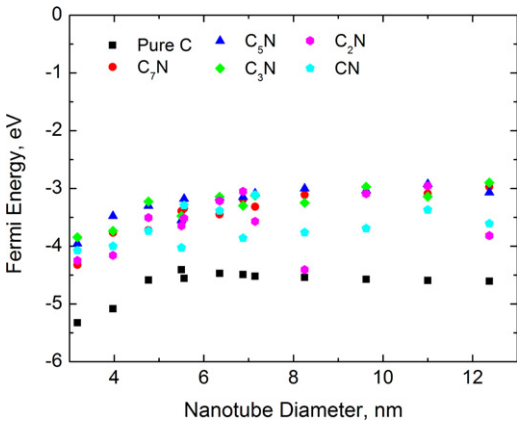

Figure 5. Calculated Fermi energy for small diameter C_xN nanotubes, over a range of $D(n, m)$.

3.4. Preliminary results of CN_x nanotubes

Finally, when undertaking a complete study of carbon nitride nanotubes, one may also ask what sort of structures may be expected when the relative concentrations of C and N is reversed, i.e.: when there is more N than C in the nanotubes. In addition to the C_xN nanotubes described above, preliminary investigations for a similar set of CN_x nanotubes were also undertaken as part of our study. In the majority of cases, analogous CN_x nanotubes (where $x = 2$, 3, 5 and 7) were found to be highly unstable, irrespective of (n, m) or substitution pattern. In some cases, the instability was so great as to disrupt the periodicity of the structure.

In a minority of cases however, there were some relaxed CN_x structures that demonstrated a reasonable degree of structural stability, and could possibly be deemed as candidates for synthesis attempts. Each of these structures exhibited uncommon morphologies which, if formed, could offer interesting functional properties. For instance, figure 6(a) shows CN_5 (6, 0) nanotube with a double helix structure, and figure 6(b) shows a CN_5 (9, 0) nanotube with a triple helix structure. These examples suggest that CN_x nanotubes may be worthy of a more detailed and systematic study in the future.

4. Conclusions

Presented in this paper are results of density functional tight-binding calculations systemically investigating the structural and thermodynamic stability of small C_xN nanotubes with $x = 1$, 2, 3, 5, and 7. The results predict that the stability of C_xN nanotubes is highly dependent on the stoichiometry and the nitrogen partial pressure (during synthesis), but is almost independent of chiral structure. Moreover, although we find that structural instabilities increase with increasing nitrogen concentration, in agreement with experimental observations [12, 11], we find that the 'patterning' of N atoms (characterized by their configurational relationship to one another) is also important in determining stability. At low N concentrations $(n, 0)$ nanotubes are more likely to retain a more perfect structure than (n, n) nanotubes, and the C_3N stoichiometry exhibits relaxed (low energy)

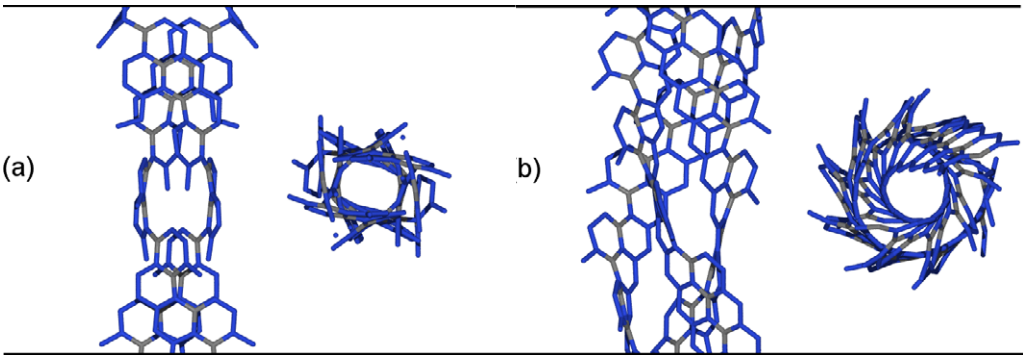

Figure 6. Although preliminary investigations found most CN_x nanotubes to be highly unstable, the relaxed (a) CN_5 (6, 0) nanotube with a double helix structure, and (b) CN_5 (9, 0) nanotube with a triple helix structure could potentially offer exploitable functional properties.

structures that appear consistently independent of chirality. At high N concentrations, neighbouring N atoms will either result in out-of-plane distortions or broken N–N bonds. However, our results indicate that protrusions characteristic of a 'winged' structure are more likely to be associated with small diameters and high N concentration than to any particular substitution pattern. These factors are considered important in developing a strategy for producing specific C_xN nanotubes, and experimentally testing the relatively constant ∼1.5 eV blue-shift we observe in the Fermi energy when $2 < x$.

Acknowledgments

This project was sponsored by the Nuffield Foundation, and the Glasstone Benefaction at the University of Oxford. Computational resources for this project have been supplied the Oxford Supercomputing Centre (OSC), and the Victorian Partnership for Advance Computing (VPAC) facility.

References

[1] Iijima S 1991 *Nature* **354** 56
[2] Saito R, Dresselhaus G and Dresselhaus M S 1998 *Physical Properties of Carbon Nanotubes* (London: Imperial)
[3] Dresselhaus M S, Dresselhaus G and Avouris P (ed) 2001 *Carbon Nanotubes, Synthesis, Structure, Properties and Applications* (Berlin: Springer)
[4] Agarwal R and Lieber C M 2006 *Appl. Phys.* A **85** 209
[5] Bockrath M, Cobden D H, Lu J, Rinzler A G, Smalley R E, Balents L and McEuen P L 1999 *Nature* **397** 598
[6] Haddon R C, Sippel J, Rinzler A G and Papadimitrakopoulos F 2004 *MRS Bull.* **29** 252
[7] Nevidomskyy A H, Csányi G and Payne M C 2003 *Phys. Rev. Lett.* **91** 105502
[8] Jang J W, Lee C E, Lyu S C, Lee T J and Lee C J 2004 *Appl. Phys. Lett.* **84** 2877
[9] Che R C, Peng L-M and Wang M S 2004 *Appl. Phys. Lett.* **85** 4753
[10] Kang H S and Jeong S 2004 *Phys. Rev.* B **70** 233411
[11] Terrones M, Redlich P, Grobert N, Trasobares S, Hsu W, Terrones H, Zhu Y, Hare J, Reeves C, Cheetham A, Rühle M, Kroto H and Walton D 1999 *Adv. Mater.* **11** 655
[12] Terrones M, Terrones H, Grobert N, Hsu W, Zhu Y, Hare J, Kroto H, Walton D, Redlich Ph, Rühle M, Zhang J and Cheetham A 1999 *Appl. Phys. Lett.* **75** 25
[13] Li J, Cao C and Zhu H 2007 *Nanotechnology* **18** 115605
[14] Miyamoto Y, Cohen M L and Louie S G 1997 *Solid State Commun.* **102** 605
[15] Porezag D, Frauenheim Th, Köhler Th, Seifert G and Kaschner R 1995 *Phys. Rev.* B **51** 12947
[16] Frauenheim Th, Seifert G, Elstner M, Niehaus Th, Köhler C, Amkreutz M, Sternberg M, Hajnal Z, Di Carlo A and Suhai S 2002 *J. Phys.: Condens. Matter* **14** 3015
[17] Sternberg M, Horner D A, Redfern P C, Zapol P and Curtiss L A 2005 *J. Comput. Theor. Nanosci.* **2** 207
[18] Barnard A S and Sternberg M 2005 *J. Phys. Chem.* B **109** 17107
[19] Barnard A S and Sternberg M 2007 *Nanotechnology* **18** 025702
[20] Barnard A S, Russo S P and Snook I K 2007 *J. Mater. Chem.* **17** 2892
[21] Trasobares S, Ewels C P, Birrell J, Stephen O, Wei B Q, Carlisle J A, Miller D, Keblinski P and Ajayan P M 2004 *Adv. Mater.* **16** 610
[22] Collins P G, Zettl A, Bando H, Thess A and Smalley R E 1997 *Science* **278** 100
[23] Xiong Y, Li Z, Guo Q and Xie Y 2005 *Inorg. Chem.* **44** 6506
[24] Lim S H, Elim H I, Gao X Y, Wee A T S, Ji W, Lee J Y and Lin J 2006 *Phys. Rev.* B **73** 045402
[25] Wu C, Zhu X, Wang C, Sheng H, Yang J and Xie Y 2007 *Appl. Phys. Lett.* **90** 113116
[26] Barnard A S and Russo S P 2003 *J. Phys. Chem.* B **107** 7577
[27] Peng L-M, Zhang Z, Xue Z, Wu Q, Gu Z and Pettifor D 2000 *Phys. Rev. Lett.* **85** 15